Attractive critical point from weak antilocalization on fractals

Sticlet, Doru; Akhmerov, Anton

DOI
10.1103/PhysRevB.94.161115

Publication date
2016

Document Version
Final published version

Published in
Physical Review B (Condensed Matter and Materials Physics)

PHYSICAL REVIEW B **94**, 161115(R) (2016)

Attractive critical point from weak antilocalization on fractals

Doru Sticlet and Anton Akhmerov
Kavli Institute of Nanoscience, Delft University of Technology, Lorentzweg 1, 2628 CJ Delft, The Netherlands
(Received 23 November 2015; published 13 October 2016)

We report an attractive critical point occurring in the Anderson localization scaling flow of symplectic models on fractals. The scaling theory of Anderson localization predicts that in disordered symplectic two-dimensional systems weak-antilocalization effects lead to a metal-insulator transition. This transition is characterized by a repulsive critical point above which the system becomes metallic. Fractals possess a noninteger scaling of conductance in the classical limit which can be continuously tuned by changing the fractal structure. We demonstrate that in disordered symplectic Hamiltonians defined on fractals with classical conductance scaling $g \sim L^{-\varepsilon}$, for $0 < \varepsilon < \beta_{\max} \approx 0.15$, the metallic phase is replaced by a critical phase with a scale-invariant conductance dependent on the fractal dimensionality. Our results show that disordered fractals allow an explicit construction and verification of the ε expansion.

DOI: 10.1103/PhysRevB.94.161115

Introduction. The one-parameter scaling hypothesis [1] is central to the study of disordered electronic systems. The hypothesis states that in disordered noninteracting systems the beta function $\beta = d \log g / d \log L$ determining the change of conductance g with the system size L is a universal function of g. Single-parameter scaling is known to be violated in quantum Hall systems [2] or topological insulators [3,4], where the topological invariant is the second scaling variable required to capture the scaling flow, and in systems where disorder itself is an irrelevant scaling variable [5–7]. Despite that, the scaling flow of Anderson localization holds in an extremely broad range of systems [8,9].

The scaling flow has two universal regimes. In the insulating regime $g \ll 1$ the exponential localization of the wave functions leads to a further decrease of conductance with the system size leading to $\beta \propto \log g + \text{constant}$. At high conductance, the beta function recovers the classical Ohm law, $\lim_{g\to\infty} \beta \equiv \beta_\infty = d - 2$ with d the Euclidean dimension. A successful prediction of the theory was the occurrence of a metal-insulator transition in $3d$ as the flow passes between these two limits. Later studies have refined the theory in the diffusive regime by taking into account quantum corrections to the Ohmic conductance [8,9]. In time-reversal-invariant systems with spin-orbit interactions, also called symplectic, the corrections to g are positive, yielding weak-antilocalization effects [10]. Consequently, these systems exhibit a metal-insulator transition even in $2d$, with logarithmic corrections to conductance $g \propto \log L$, and a metallic phase at large conductance (see Fig. 1).

A successful approach in treating Anderson localization is the ε expansion, which treats d as a continuous variable and constructs a series expansion of the scaling flow [11–14]. The ε expansion is a mathematical construct which is not expected to have a physical meaning when d is not integer; nevertheless, fractals are examples of systems with noninteger dimensionality. This motivates the main question of our work: Does the scaling hypothesis hold on fractals? The scaling theory of phase transitions on fractals holds for the Ising model [15,16], the percolation transition [17], as well as the metal-insulator transition of the Anderson model on bifractal lattices [18,19]. Tangential to our study are the investigations of shot noise in fractal resistor networks [20,21] and quantum transport on clean Sierpiński gaskets [22–24] and carpets [25].

If the scaling hypothesis does hold, the simplest possible modification of the scaling flow on the fractal would be an overall shift of β such that β_∞ matches the properties of the Ohm law on a fractal. This leads us to the following prediction: There exist fractals such that the scaling flow of a symplectic model on them has a metal-insulator transition and an attractive critical point (shown in Fig. 1). The appearance of this type of critical point on fractals is a unique property of Anderson scaling flow in symmetry classes allowing weak antilocalization, and it constitutes the main focus of our study. Until now it has not been observed, despite numerical studies which confirmed the presence of the usual metal-insulator transition on symplectic fractals with Hausdorff dimension lower than two [26].

Analytical arguments for the presence of two critical points. Physical observables obey anomalous scaling laws in fractal systems; see Refs. [27–29] for reviews. Instead of the Euclidean dimension d of the embedding space, these scaling laws are governed by the Hausdorff and the spectral dimension. The Hausdorff dimension d_h determines the scaling of the volume occupied by the fractal. The spectral (fracton) dimension d_s characterizes scaling of the low-energy density of states of the Laplace operator on the fractal $\rho(\omega) \propto \omega^{d_s/2-1}$ [30], and therefore is relevant to diffusion and phonon dispersion on fractals. While for Euclidean systems the exponents d, d_h, and d_s are identical, in fractals they obey the inequality $d \geqslant d_h \geqslant d_s$ [31].

The insulating limit of the scaling flow is governed by the exponential localization of wave functions on almost decoupled orbitals, and applies whenever the growth of the number of nth nearest neighbors of an orbital is subexponential with n. Therefore the scaling on fractals should hold in the insulating limit $g \ll 1$. The classical limit $g \gg 1$ is governed by a diffusion equation. Diffusion on fractals is slowed down so that the mean-square displacement of a random walker on fractals reads $\langle r^2 \rangle \propto t^\gamma$, with the subdiffusion exponent $\gamma = d_s/d_h < 1$ [30,32]. The Einstein relation links the diffusion and conductivity, and yields the scaling of diffusive conductance on fractals [28,31,33]:

$$g_0 \propto L^{\beta_\infty}, \quad \beta_\infty = d_h - 2d_h/d_s. \tag{1}$$

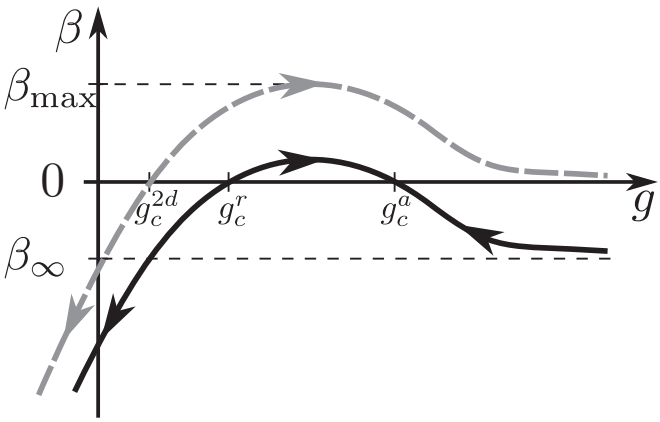

FIG. 1. The conductance flow ($\beta = d \log g/d \log L$) as a function of dimensionless conductance g. There is a single repulsive critical point at $g = g_c^{2d}$ for symplectic systems in $2d$ (dashed gray line). The conjectured flow for symplectic fractals with Hausdorff dimension lower than two (solid black line) can display an attractive critical point g_c^a, in addition to the usual repulsive point g_c^r. The fractal is insulating in the diffusive limit, with a negative offset β_∞ due to the fractal Ohm law.

In particular, Ref. [31] makes an observation that Eq. (1) agrees with the scaling hypothesis of Anderson localization similarly to the classical diffusive conductance on Euclidean lattices.

If the scaling conjecture holds for conductance in fractal systems, then its asymptotic form at $g \gg 1$ should be

$$\beta = \beta_\infty + A/g + O(g^{-2}), \tag{2}$$

with β_∞ the fractal diffusive conductance scaling exponent and $A \sim O(1)$ a scale-independent constant whose sign depends on the symmetry class of the problem. In particular, this scaling form was postulated [34] for the orthogonal symmetry class. We verify that the scaling hypothesis holds at least in the $g \gg 1$ limit by using the return probability $p_0(t)$ after a time t [35–38] and the fractal diffusion equation. In a fractal lattice the return probability is a function of d_s, $p_0(t) \propto t^{-d_s/2}$ [31,39]. Therefore the conductance correction δg to the fractal Ohm law reads

$$\frac{\delta g}{g_0} \propto \int_0^\infty dt\, p_0(t) e^{-t/\tau_\phi} \propto \tau_\phi^{1-d_s/2}, \tag{3}$$

with τ_ϕ the phase-coherence time. Calculating the prefactor of the integral is beyond the scope of our work. It depends on fractal dimensions, but it is always positive for a Hamiltonian in the symplectic class. Replacing τ_ϕ with the typical time it takes a random walker to escape the system $L^2 \propto \tau_\phi^{d_s/d_h}$, and using the definition of the scaling exponent Eq. (1), we conclude that the quantum correction to scaling is a scale-independent constant g_c, unlike a divergent correction $\delta g \propto \log L$ in $2d$. Therefore the scaling function, calculated from the asymptotic form of conductance $g(L) = g_0 + g_c$, reads

$$\beta = \beta_\infty - \beta_\infty g_c/g. \tag{4}$$

For weak antilocalization, the correction to the flow is positive; from Eq. (2) $A = -\beta_\infty g_c > 0$, since β_∞ is negative. We observe that indeed, the scaling of conductance is satisfied also by the fractal diffusion equation.

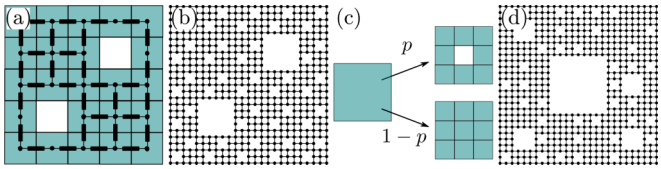

FIG. 2. Fractal patterns where we observe two critical points. (a) Sierpiński 5×5 pattern and (b) two-level lattice created using the pattern. The fractal pattern is mapped to resistor networks (black rectangles denote resistors). (c) Decimation procedure to create statistical fractals derived from 3×3 Sierpiński patterns and (d) a three-level lattice with $p = 0.5$. For statistical fractals, at any decimation step, there is a probability p that a lattice block is carved with the fractal pattern. The lattice turns from Euclidean ($p = 0$) to regular fractal ($p = 1$) by continuous variation of p.

When β_∞ is negative and close to 0, $\beta_\infty < 0$ and $|\beta_\infty| \ll 1$, the scaling function (4) vanishes at $g_c = -A/\beta_\infty \gg 1$. Since higher order quantum corrections to scaling $\delta g = O(g^{-2})$ should be negligible when $g \gg 1$, the second critical point must indeed appear, and it has to be attractive, as shown in Fig. 1. In the following, numerical simulations will support this prediction by tuning β_∞ using different fractal geometries.

Choice of the fractal. The parameters of a fractal with two critical points are limited by two considerations. On the one hand, if $|\beta_\infty|$ is too large, the quantum corrections to scaling become insufficiently strong to create a zero of the β function. Assuming that the main effect of changing the fractal exponents is an overall shift of the β function provides the requirement $|\beta_\infty| < \beta_{\max}$, with $\beta_{\max} \approx 0.15$, the maximum [40] of the β function in a symplectic $2d$ model. On the other hand, β_∞ must be negative for the second critical point to appear. If β_∞ approaches either of the limiting values, the scaling flow near the attractive critical point slows down, complicating the observation of criticality. Additionally, when β_∞ is close to zero, the attractive critical point occurs at large conductance g, requiring large system sizes, which are impractical for numerical simulations. We therefore choose to use a fractal with $\beta_\infty \approx -0.1$.

In order to tune β_∞, we consider two generalizations of Sierpiński carpets. In the first case, the fractal remains regular, with a number of subdivisions, larger than 3×3 [see Figs. 2(a) and 2(b)]. In the second case, statistical fractals are generated using a probabilistic subdivision rule, where the central subblock is removed with a probability p [see Figs. 2(c) and 2(d)].

Varying the number and position of removed cells in each subdivision or changing p allows us to control d_h and d_s. In order to compute β_∞, we construct finite-size versions of each fractal, replace the centers of each cell with nodes of a resistor network, and connect neighboring nodes with equal resistors, as shown in Fig. 2(a). We set the potential of the leftmost modes to 0, and that of the rightmost to 1, and numerically solve the resulting Kirchhoff equations for several system sizes and geometric disorder realizations in the case of statistical fractals [41]. The Kirchoff system of equations is defined and solved using the Kwant package [42]. Finally, the length-independent β_∞ follows by fitting the finite-size fractal

results dependent on average $g(L)$ to

$$\beta_{\text{classical}}(L) \equiv \log_b \frac{\langle g(L)\rangle}{\langle g(L/b)\rangle} = \beta_\infty + cL^{-\mu}, \qquad (5)$$

with b, the pattern magnification factor, and c and μ constants.

This procedure yields results which agree with the exact value of β_∞ for a Sierpiński gasket [41]. For the classical 3×3 Sierpiński carpets, which lacks exact analytic results [43], we determine numerically $\beta_\infty \approx -0.2$, which lies within the bounds provided by the approximate renormalization group analysis [44–46]. This result also means that classical Sierpiński fractals will not host two critical points, which was a reason to search for alternative patterns. We find that the suitable value $\beta_\infty \approx -0.1$ is reached by the recursion pattern shown in Fig. 2(a) and statistical Sierpiński carpets with $p = 0.5$. From resistor network simulations [41], we extract the classical conductance exponent in the 5×5 pattern with $d_h = \log_5(23)$: $\beta_\infty \approx -0.1055$. In the $p = 0.5$ statistical fractal with Hausdorff dimension $\bar{d}_h = \log_3(8.5)$, after averaging conductance for an ensemble of 10^4 geometrically disordered lattices at each L, we find $\beta_\infty \approx -0.1063$ [41].

Quantum simulations of symplectic fractals. We investigate the scaling flow on fractals using the tight-binding Ando Hamiltonian [47,48]

$$H = \sum_{\boldsymbol{r}} \left[V_{\boldsymbol{r}} c^\dagger_{\boldsymbol{r}} \sigma_0 c_{\boldsymbol{r}} - t \sum_{\boldsymbol{r}' \in \text{nn}} c^\dagger_{\boldsymbol{r}'} e^{i\theta(\boldsymbol{r}'-\boldsymbol{r})\cdot\boldsymbol{\sigma}} c_{\boldsymbol{r}} \right], \qquad (6)$$

defined on sites $\boldsymbol{r}$ of a finite-order fractal cut out of a square lattice with unit lattice constant, with $c^\dagger_{\boldsymbol{r}}$ and $c_{\boldsymbol{r}}$ the electron creation and annihilation operators. Here σ are the Pauli matrices acting in spin space, and $\theta = \pi/6$ is the spin-orbit coupling parameter. The hoppings with amplitude $t = 1$ are connecting the sites with their nearest neighbors on a square lattice, if those are present in the fractal. The random uncorrelated on-site potential $V_{\boldsymbol{r}}$ is uniformly distributed in the interval $[-V/2, V/2]$, with V the disorder strength. We attach leads to the leftmost and rightmost sites present in the system, and compute conductance using the Kwant package [42,43].

We calculate the average conductance as a function of disorder strength and fractal size. Our results for the fractal of Fig. 2(a) are shown in Fig. 3(a) for the sizes $L = 125$ and $L = 625$. The corresponding data for the fractal of Fig. 2(c) with $p = 0.5$ and fractal sizes 81, 243, and 729 are presented in the Supplemental Material [41] and exhibit the same trends. We find that the conductance grows with size for intermediate disorder strengths, and drops both for high and low disorder. The crossing of the curves at large disorder strength is the usual repulsive critical point marking the transition towards the strongly localized phase at $g < g^r_c$ [26]. The crossing of conductance curves at lower disorder strength realizes the attractive critical point g^a_c. We fit the $g(L)$ in the vicinity of the attractive critical point with $g(L) = g^a_c + c(V - V_c)L^{1/\nu_a}$, with V_c, the critical disorder, ν_a, the critical exponent, and c a constant. The resulting values are $1/\nu_a = -0.0668 \pm 0.00006$, $g^a_c = 3.811 \pm 0.002$ for the deterministic fractals, while for the statistical ones [41], $1/\nu_a = -0.0847 \pm 0.0005$ and $g^a_c = 3.598 \pm 0.026$ (for $L = 243{,}729$ lattices). There are several sources of error which account for observed deviation of ν_a from the prediction given in Eq. (4) $1/\nu_a = \beta_\infty$.

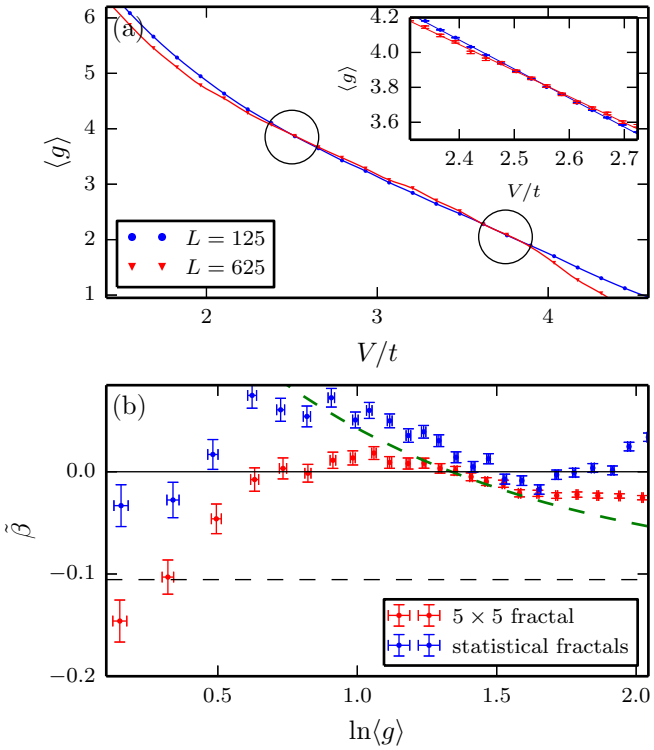

FIG. 3. (a) Quantum transport results for a 5×5 pattern Sierpiński carpet. Average dimensionless conductance g as a function of disorder strength. There are two critical points (encircled) and an intermediate metallic scaling regime. There are 10^4 disorder realizations for $L = 125$ lattice, and 10^3, for $L = 625$. The lines represent a cubic interpolation of experimental points (markers) to guide the eye. The inset shows a zoom at g^a_c, where there are 10^5 disorder realization for $L = 125$ and 5×10^3, for $L = 625$. The critical exponent is extracted from a linear fit of conductance curves near g^a_c (inset lines). The error bars represent the root-mean-square deviation. (b) Approximate scaling function $\tilde{\beta}$ for 5×5 fractals (red) and for the largest lattice sizes in statistical fractals $L = 243{,}729$ (blue). The green dashed line is the prediction of Eq. (4) with g^a_c from 5×5 pattern simulations. The dashed black line denotes β_∞.

Specifically, the $O(g^{-2})$ corrections to the scaling function due to strong localization should make $|\nu_a|$ larger, while the finite-size corrections due to a finite mean free path may affect the obtained value of ν_a either way.

Since the numerics limits the system sizes to only two or three values, we calculate the approximate β function $\tilde{\beta} = \log[g(L_2)/g(L_1)]/\log(L_2/L_1)$, with L_2 the largest available system size, and $L_1 = L_2/b$. This approximation is appropriate despite b not being infinitesimally small since the conductance only changes slowly with length. On the other hand, separating the finite-size corrections to the β function requires more system sizes and larger computational resources. The dependence of $\tilde{\beta}$ on $[g(L_2) + g(L_1)]/2$ is shown in Fig. 3(b) for both fractal types that we study. We observe that both curves agree with the predicted qualitative scaling flow, and show a clear presence of two critical points. Also in agreement with our expectations, the deviations from the predictions of weak antilocalization become significant not only at small

conductance, due to strong localization, but also at large conductance, due to the increase of mean free path and finite-size effects.

Summary. We presented analytical arguments for the scaling hypothesis validity on fractals, and showed that the competition between the positive quantum corrections to conductance and the diffusive conductance scaling can lead to the occurrence of an additional attractive critical point. By tuning the fractal dimensions to the optimal regime with $\beta_\infty \approx -0.1$, we have also observed this critical point using numerical simulations. Our findings are an example of the appearance of phases on fractals that cannot be observed in integer dimensions.

While the main relevance of our work is theoretical, the scaling of conductance can be observed experimentally using a patterned low effect mass quantum well with high spin-orbit coupling such as InAs or InSb at ultralow temperatures. With spin-orbit length $l_{SO} \approx 100\,nm$ at these structures, it becomes possible to aim for a 30 nm feature size, while the dephasing length can be on the order of microns at the lowest accessible temperatures. A natural further question to investigate is how the multifractal properties of the wave functions at the critical point are tied to the fractal dimensions d_h and d_s of the parent fractal. Our work can be straightforwardly adapted to other symmetry classes supporting weak antilocalization, such as the thermal metal phase characterized by the presence of particle-hole symmetry and absence of time reversal. Finally, we expect that further analytical progress is possible using d-dimensional Sierpiński gaskets due to their finite ramification. When $d \to \infty$, the conductance scaling β_∞ of Sierpiński gaskets asymptotically approaches 0, offering a way to analyze localization in regular $2d$ lattices.

Acknowledgments. We thank Yuval Oreg for drawing our attention to the topic, and Adriaan Vuik for code revision. This research was supported by the Foundation for Fundamental Research on Matter (FOM), the Netherlands Organization for Scientific Research (NWO/OCW) as part of the Frontiers of Nanoscience program, and an ERC Starting Grant No. 638760.

[1] E. Abrahams, P. W. Anderson, D. C. Licciardello, and T. V. Ramakrishnan, Phys. Rev. Lett. **42**, 673 (1979).
[2] D. E. Khmel'nitskiĭ, Pis'ma Zh. Eksp. Teor. Fiz. **38**, 454 (1983) [J. Exp. Theor. Phys. **38**, 552 (1984)].
[3] R. S. K. Mong, J. H. Bardarson, and J. E. Moore, Phys. Rev. Lett. **108**, 076804 (2012).
[4] A. Altland, D. Bagrets, and A. Kamenev, Phys. Rev. B **91**, 085429 (2015).
[5] A. Altland and D. Bagrets, Phys. Rev. Lett. **114**, 257201 (2015).
[6] S. V. Syzranov, V. Gurarie, and L. Radzihovsky, Phys. Rev. B **91**, 035133 (2015).
[7] M. Gärttner, S. V. Syzranov, A. M. Rey, V. Gurarie, and L. Radzihovsky, Phys. Rev. B **92**, 041406 (2015).
[8] P. A. Lee and T. V. Ramakrishnan, Rev. Mod. Phys. **57**, 287 (1985).
[9] F. Evers and A. D. Mirlin, Rev. Mod. Phys. **80**, 1355 (2008).
[10] S. Hikami, A. I. Larkin, and Y. Nagaoka, Prog. Theor. Phys. **63**, 707 (1980).
[11] L. P. Gorkov, A. I. Larkin, and D. E. Khmel'nitskiĭ, Pis'ma Zh. Eksp. Teor. Fiz. **30**, 248 (1979) [JETP Lett. **30**, 228 (1979)].
[12] F. Wegner, Z. Phys. B **35**, 207 (1979).
[13] E. Abrahams and T. V. Ramakrishnan, J. Non-Cryst. Solids **35–36**, 15 (1980).
[14] F. Wegner, Z. Phys. B **36**, 209 (1980).
[15] Y. Gefen, B. B. Mandelbrot, and A. Aharony, Phys. Rev. Lett. **45**, 855 (1980).
[16] Y. Gefen, Y. Meir, B. B. Mandelbrot, and A. Aharony, Phys. Rev. Lett. **50**, 145 (1983).
[17] S. Havlin, D. Ben-Avraham, and D. Movshovitz, Phys. Rev. Lett. **51**, 2347 (1983).
[18] M. Schreiber and H. Grussbach, Phys. Rev. Lett. **76**, 1687 (1996).
[19] I. Travěnec and P. Markoš, Phys. Rev. B **65**, 113109 (2002).
[20] R. Rammal, C. Tannous, and A.-M. S. Tremblay, Phys. Rev. A **31**, 2662 (1985).
[21] C. W. Groth, J. Tworzydło, and C. W. J. Beenakker, Phys. Rev. Lett. **100**, 176804 (2008).
[22] A. Chakrabarti, J. Phys.: Condens. Matter **8**, 10951 (1996).
[23] Y. Liu, Z. Hou, P. M. Hui, and W. Sritrakool, Phys. Rev. B **60**, 13444 (1999).
[24] Z. Lin, Y. Cao, Y. Liu, and P. M. Hui, Phys. Rev. B **66**, 045311 (2002).
[25] E. van Veen, A. Tomadin, M. I. Katsnelson, S. Yuan, and M. Polini, Phys. Rev. B **93**, 115428 (2016).
[26] Y. Asada, K. Slevin, and T. Ohtsuki, Phys. Rev. B **73**, 041102 (2006).
[27] M. B. Isichenko, Rev. Mod. Phys. **64**, 961 (1992).
[28] T. Nakayama, K. Yakubo, and R. Orbach, Rev. Mod. Phys. **66**, 381 (1994).
[29] B. B. Mandelbrot, *The Fractal Geometry of Mature* (W. H. Freeman, San Francisco, 1982).
[30] S. Alexander and R. Orbach, J. Phys. Lett. **43**, 625 (1982).
[31] R. Rammal and G. Toulouse, J. Phys. Lett. **44**, 13 (1983).
[32] Y. Gefen, A. Aharony, B. B. Mandelbrot, and S. Kirkpatrick, Phys. Rev. Lett. **47**, 1771 (1981).
[33] D. Ben-avraham, S. Havlin, and D. Movshovitz, Philos. Mag. B **50**, 297 (1984).
[34] Y. Gefen, D. J. Thouless, and Y. Imry, Phys. Rev. B **28**, 6677 (1983).
[35] A. I. Larkin and D. E. Khmel'nitski, Sov. Phys. Usp. **25**, 185 (1982).
[36] G. Bergmann, Phys. Rep. **107**, 1 (1984).
[37] S. Chakravarty and A. Schmid, Phys. Rep. **140**, 193 (1986).
[38] C. W. J. Beenakker and H. van Houten, in *Solid State Physics*, Semiconductor Heterostructures and Nanostructures, Vol. 44, edited by Henry Ehrenreich and David Turnbull (Academic Press, New York, 1991), pp. 1–228.
[39] B. O'Shaughnessy and I. Procaccia, Phys. Rev. Lett. **54**, 455 (1985).
[40] Y. Asada, K. Slevin, and T. Ohtsuki, Phys. Rev. B **70**, 035115 (2004).
[41] See Supplemental Material at http://link.aps.org/supplemental/10.1103/PhysRevB.94.161115 for source code and the resulting data.

[42] C. W. Groth, M. Wimmer, A. R. Akhmerov, and X. Waintal, New J. Phys. **16**, 063065 (2014).

[43] Ramification of a fractal measures the smallest number of bonds needed to be severed in order to detach any self-similar set from the rest of the network. The Sierpiński carpets have infinite ramifications since the connections of a self-similar set to the rest of the lattice grow with the size of its border. If the ramification order is finite, it is possible to devise exact renormalization group techniques to determine the scaling of different physical observables. This is the case for Sierpiński gaskets, where block renormalization yields $\beta_\infty = \log_2(3/5) \approx -0.74$.

[44] Y. Gefen, A. Aharony, and B. B. Mandelbrot, J. Phys. A: Math. Gen. **17**, 1277 (1984).

[45] S. Havlin, D. Ben-Avraham, and D. Movshovitz, J. Stat. Phys. **36**, 831 (1984).

[46] Y.-k. Wu and B. Hu, Phys. Rev. A **35**, 1404 (1987).

[47] S. N. Evangelou and T. Ziman, J. Phys. C **20**, L235 (1987).

[48] T. Ando, Phys. Rev. B **40**, 5325 (1989).